Electronic Supplementary Material (ESI) for ChemComm.

Electronic Supplementary Information

Efficient visible light-driven water oxidation catalysed by an iron(IV) clathrochelate complex

Sergii I. Shylin,*[a] Mariia V. Pavliuk,[a] Luca D'Amario,[a] Fikret Mamedov,[a] Jacinto Sá,[a] Gustav Berggren [a] and Igor O. Fritsky*[b]

[a] Department of Chemistry – Ångström Laboratory, Uppsala University, P.O. Box 523, 75120 Uppsala, Sweden. E-mail: sergii.shylin@kemi.uu.se
[b] Department of Chemistry, Taras Shevchenko National University of Kyiv, Volodymyrska 64, 01601 Kiev, Ukraine. E-mail: ifritsky@univ.kiev.ua

Table of Contents

Experimental Procedures

Materials.

All of the reagents and solvents were purchased from commercial sources and used without further purification. $[Ru(bpy)_3](ClO_4)_2$ was prepared by anion exchange from $[Ru(bpy)_3]Cl_2$ (Aldrich) and recrystallised from ethanol. $[Ru(bpy)_3](ClO_4)_3$ was prepared from $[Ru(bpy)_3](ClO_4)_2$ as described previously [1]. Distilled water was additionally purified using a Milli-DI water purification system.

Synthesis of $Na_2[Fe^{IV}(L{-}6H)]\cdot 2H_2O$ *(**1**).*

Formaldehyde, 37 % (0.67 ml, 9 mmol) was mixed with the solution of NaOH (0.2 g, 5 mmol) in 5 ml of water. The resulting mixture was heated up to 90 °C and rapidly added to the warm solution containing $Fe(ClO_4)_3\cdot H_2O$ (0.372 g, 1 mmol) and oxalodihydrazide (0.354 g, 3 mmol) in 15 ml of water. The reaction mixture acquired a green colour in a few minutes. It was stirred for 2 h at ambient temperature, filtered off, and water from the filtrate was removed on a rotary evaporator. The resulting dark green powder was washed with chloroform (30 ml), then with ethanol (10 ml), and air dried. The powder was dissolved in 10 ml of warm (70 °C) water, filtered off, and the solution was cooled to 4 °C. In 24 h this yielded dark green powder of **1** that was filtered off and air dried. Yield 47.2 mg (8.4 %). Elemental analysis for $C_{12}H_{16}N_{12}O_8Na_2Fe$: calculated, %: C, 25.82; H, 2.89; N, 30.11. Found, %: C, 25.97; H, 3.03; N, 29.92. The main FTIR bands: 3415 cm^{-1} (s), 2951 cm^{-1} (m), 1642 cm^{-1} (s), 1611 cm^{-1} (s), 1429 cm^{-1} (m), 1391 cm^{-1} (m), 1383 cm^{-1} (m), 1299 cm^{-1} (m), 1201 cm^{-1} (m), 1110 cm^{-1} (m), 1093 cm^{-1} (m), 1028 cm^{-1} (m), 896 cm^{-1} (m).

Electrochemical analysis.

Cyclic voltammetry was carried out by using an Autolab potentiostat with a GPES electrochemistry interface (Eco Chemie). A three-electrode system with a 3 mm glass carbon working electrode, a glassy carbon rod counter electrode, and an Ag/AgCl (with saturated KCl aqueous solution) reference electrode was used. The counter and reference electrodes were in compartments separated from the bulk solution by fritted disks. The working electrode was polished with 0.05 μm alumina paste and sonicated before use. The solution under study (6 ml) contained **1** (0.25 mM), borate buffer (0.1 M, pH 8.0) and $KClO_4$ (0.1 M) as a supporting electrolyte. Before all measurements, oxygen was removed from the cell by bubbling argon through the stirred solutions. Samples were kept under argon during the measurements.

Oxygen evolution experiments.

A standard Clark electrode (Hansatech Instruments) equipped with a water thermostat was used for oxygen detection. The electrode was separated from the sample solution by a Teflon membrane, and the signal was recorded using the Oxygraph software package. Air-saturated aqueous solution ($[O_2]_{20\,°C}$ = 276 μm) was used for calibration of the electrode [2]. All experiments were done at 20 °C. The cell was purged with argon gas before each experiment, and the solution in the cell (1 ml) was continuously stirred. Visible light LEDs (λ = 450(10) nm, 820 μE cm^{-2} s^{-1}) were used as illumination sources in the photoinduced reactions. Prior to water oxidation studies, the concentration of photosensitiser $[Ru(bpy)_3](ClO_4)_2$ was varied to optimise the reaction conditions. The catalytic system showed the highest performance in the $[Ru(bpy)_3](ClO_4)_2$ concentration range of 0.1–0.3 mM.

In a typical oxygen evolution experiment, the solution in the working cell contained $[Ru(bpy)_3](ClO_4)_2$ (0.2 mM), $Na_2S_2O_8$ (2 mM) in borate buffer (0.1 M, pH 8.0 unless otherwise noted), and concentration of **1** was varied in the range 0.1 – 2.0 μM. To demonstrate that oxygen is evolved by the integral catalytic system, a set of control measurements was performed. Oxygen evolution traces observed in the absence of one of the key components ($[Ru(bpy)_3](ClO_4)_2$, or $Na_2S_2O_8$, or **1**) are shown in Figure S13. Chemical water oxidation was performed by adding an aqueous solution of **1** to the chemical oxidant $[Ru(bpy)_3](ClO_4)_3$ (1 mM) solution in borate buffer (0.1 M, pH 8.0) in darkness. The TON value was calculated as number of oxygen molecules evolved by one molecule of **1** by the moment of time, when reaction rate decreased to zero. The TOF value was calculated as number of oxygen molecules evolved by one molecule of **1** per second as the slope of the linear dependence of the reaction rate on concentration of **1**.

Steady-state UV-Vis absorption spectroscopy.

The UV-Vis spectra were recorded using Varian Cary 50 spectrometer in a 1 mm cuvette. For the Fe^{V} generation studies shown in Figure 4 in the main text, the aqueous solution containing $[Ru(bpy)_3](ClO_4)_2$ (0.2 mM), $Na_2S_2O_8$ (2 mM), and **1** (0.02 mM) in borate buffer (0.1 M, pH 8.0) was illuminated using visible light LEDs (λ = 450(10) nm) during 20 s. For the $[Ru(bpy)_3]^{2+}$ oxidation studies, conditions are given in the caption of Figure S7. For the chemical oxidation of Fe^{IV} by using Ru^{III}, conditions are given in the caption of Figure S9. Stability of **1** at pH 8.0 was demonstrated by UV-Vis spectra of the buffered solution of **1** (0.02 mM) kept in a closed quartz cuvette at room temperature over 3 months (Figure S14).

Time-resolved UV-Vis absorption spectroscopy.

Advanced time-resolved experiments were carried out on laser based spectroscopy as described recently [3]. The solutions under study were measured in a 1 mm quartz cuvette using pump-probe methodology. Microsecond transient absorption kinetics were recorded by a Q-switched Nd:YAG laser (Quanta Ray Pro-230), which produced a tripled frequency pulses with $\lambda = 355$ nm (13 ns). The laser was coupled with an optical parametric oscillator to obtain the desired wavelength (460 nm) for the pump light. The excitation light power of 30 mJ per pulse was used in all experiments. The data were collected using an Edinburgh Instruments LP900 spectrometer equipped with a 450 W Xe lamp used as a probe light source. Light was collected by using an Andor CCD camera for TA spectra and a R928 photomultiplier tube (Hamamatsu) for kinetic traces.

Kinetic traces of the optical density at 420 nm (shoulder of the absorption band of $[Ru(bpy)_3]^{2+}$) were studied for two solutions. Both contained $[Ru(bpy)_3](ClO_4)_2$ (0.04 mM) and $Na_2S_2O_8$ (0.4 mM) at pH 8.0, and one of the solution contained **1** (0.002 mM). The kinetic trace for the latest solution was fitted using exponential decay $\Delta OD(t) = a \cdot \exp(-t/\tau)$, where τ is a lifetime of the transient state.

DLS measurements.

DLS experiments were performed by using a Zetasizer Nano S scattering system (Malvern Instruments) that uses a uni-phase He-Ne laser (633 nm; 4 mW) working in cross auto-correlation mode. The scattering angle was set to 90° in respect the incident laser. The intensity correlation curves were analysed with the Zetasizer family software. The size measurement range was 0.3 nm – 10 µm.

EPR spectroscopy.

X-band EPR spectra were recorded on a Bruker ELEXSYS E580 spectrometer equipped with an Oxford liquid helium cryostat and an ITC4 temperature controller at 5 K. The microwave power was 10 mW, modulation amplitude was 10 G, and the microwave frequency was 9.63 GHz. All data acquisition was carried out by the Bruker Xepr software. The spectra of the solution containing $[Ru(bpy)_3](ClO_4)_2$ (0.5 mM), $Na_2S_2O_8$ (2 mM), and **1** (0.2 mM) in borate buffer (0.1 M, pH 8.0) were recorded before and after illumination at 450 nm (LEDs) during 20 s. The spectrum of $[Ru(bpy)_3]^{3+}$ was obtained after illumination at 450 nm during 20 s of the solution containing $[Ru(bpy)_3](ClO_4)_2$ (0.5 mM) and $Na_2S_2O_8$ in borate buffer (0.1 M, pH 8.0).

Mössbauer spectroscopy.

^{57}Fe Mössbauer spectra of the powdered sample and frozen aqueous solution (^{57}Fe-enriched, 20%) were recorded with a ^{57}Co source (~100 mCi) embedded in a Rh matrix using a constant acceleration Mössbauer spectrometer (Wissel) equipped with a liquid nitrogen cryostat at 80 K. Fitting of the experimental data was performed with Recoil software [4]. Hyperfine parameters uncertainties were evaluated from the covariance matrix of the fit. Isomer shifts are given relatively to iron metal at ambient temperature.

Other methods.

Elemental analyses (CHN) was performed using PerkinElmer 2400 analyser. FTIR spectra were recorded in KBr pellets using Bruker 113v spectrometer in the 400–4000 cm^{-1} region. ESI mass spectra were recorded using Bruker micrOTOF focus II system.

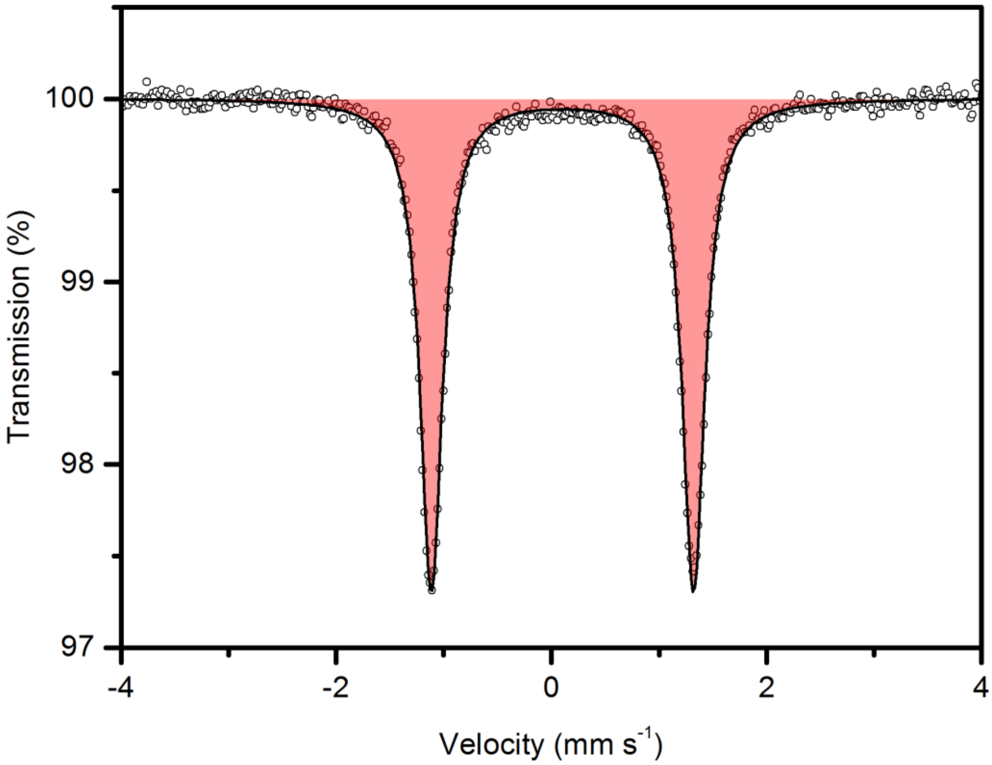

Fig. S1 ^{57}Fe Mössbauer spectrum of $Na_2[Fe^{IV}(L–6H)]\cdot 2H_2O$ (**1**) recorded at 80 K: experimental data (open circles) and fit (solid line) with hyperfine parameters $\delta = 0.118(2)$ mm s^{-1} and $|\Delta E_Q| = 2.493(3)$ mm s^{-1}. The parameters are consistent with those reported previously for $(C_6N_4H_{13})_2[Fe^{IV}(L–6H)]\cdot 5H_2O$ ($\delta = 0.116(2)$ mm s^{-1} and $|\Delta E_Q| = 2.495(4)$ mm s^{-1}) and $(Ph_4As)_2[Fe^{IV}(L–6H)]\cdot 13.28H_2O$ ($\delta = 0.121(3)$ mm s^{-1} and $|\Delta E_Q| = 2.505(5)$ mm s^{-1}) at 80 K [5].

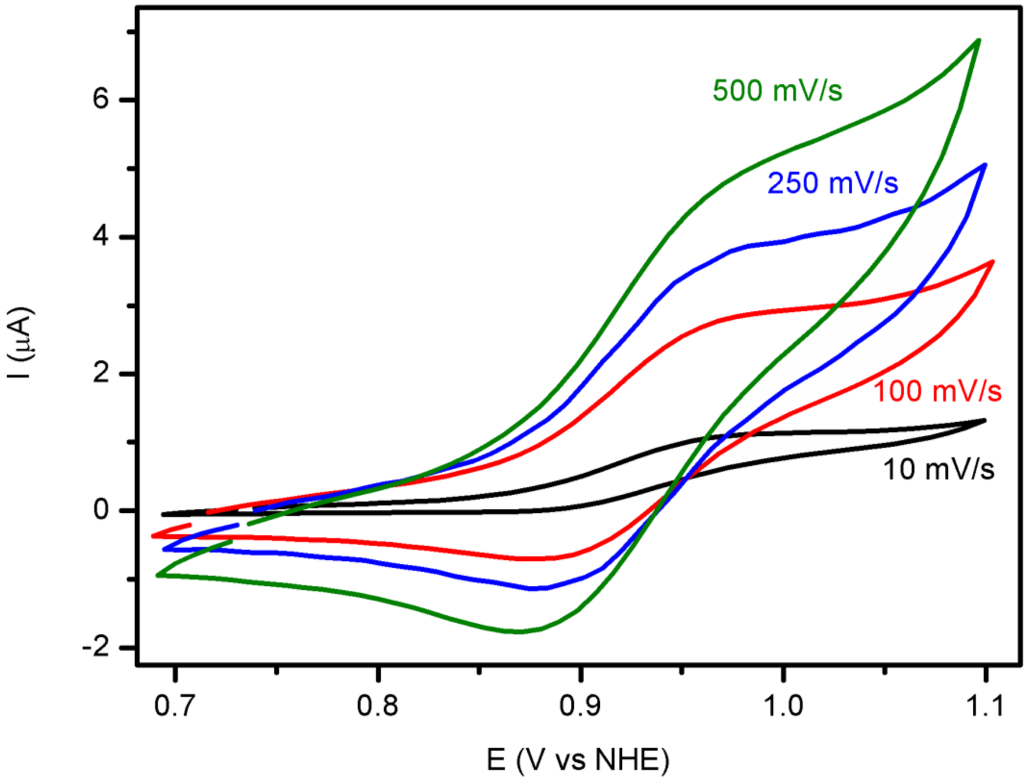

Fig. S2 Cyclic voltammograms of **1** at pH 8.0 recorded at different scan rates showing oxidation (E = 0.97 V vs NHE) and reduction (E = 0.87 V vs NHE) processes corresponding to the Fe^{V}/Fe^{IV} redox couple.

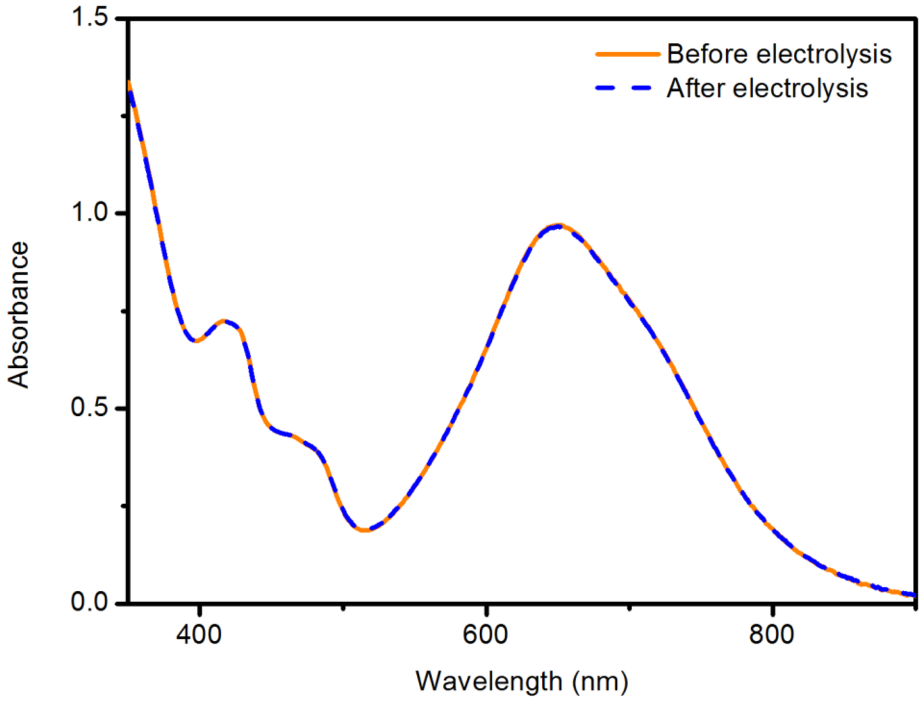

Fig. S3 UV-Vis absorption spectra of **1** (0.1 mM) in borate buffer (0.1 M) with addition of supporting electrolyte $KClO_4$ (0.1 M) recorded before and 2 h after controlled potential electrolysis at 1.4 V versus NHE with sustained current of 80–90 μA. The spectra show no decrease in concentration of **1** upon electrolysis over 2 h.

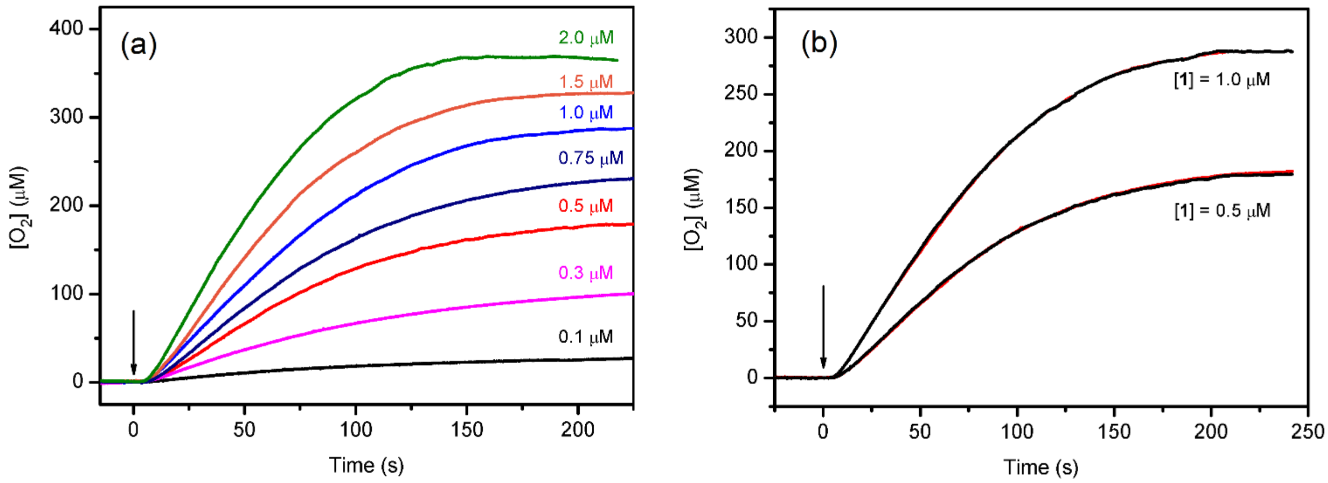

Fig. S4 (a) Traces of oxygen evolution obtained using Clark electrode for the catalytic systems containing $[Ru(bpy)_3](ClO_4)_2$ (0.2 mM), $Na_2S_2O_8$ (2 mM), and **1** (0.1–2.0 μM) in borate buffer (0.1 M, pH = 8). Arrow indicates start of illumination at 450 nm (LEDs).

(b) Selected oxygen evolution traces showing reproducibility of the TON and TOF (black – 1st run; red – 2nd run).

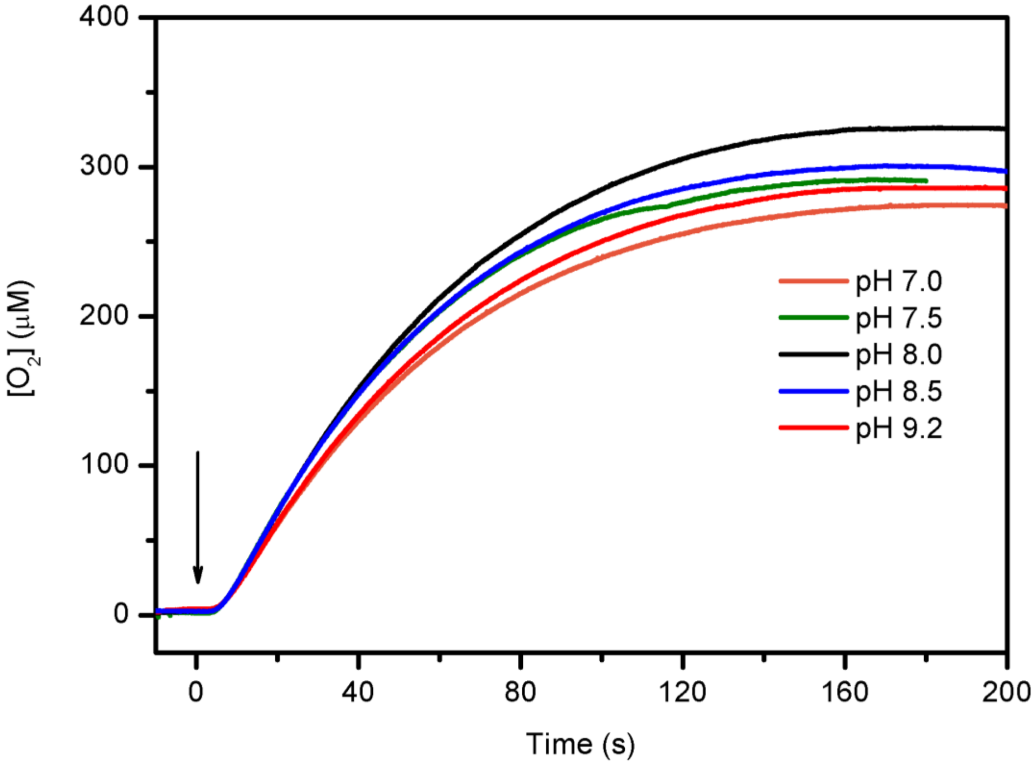

Fig. S5 Traces of oxygen evolution obtained using Clark electrode for the catalytic systems containing $[Ru(bpy)_3](ClO_4)_2$ (0.2 mM), $Na_2S_2O_8$ (2 mM), and **1** (1.5 μM) at different pH. Arrow indicates start of illumination at 450 nm (LEDs).

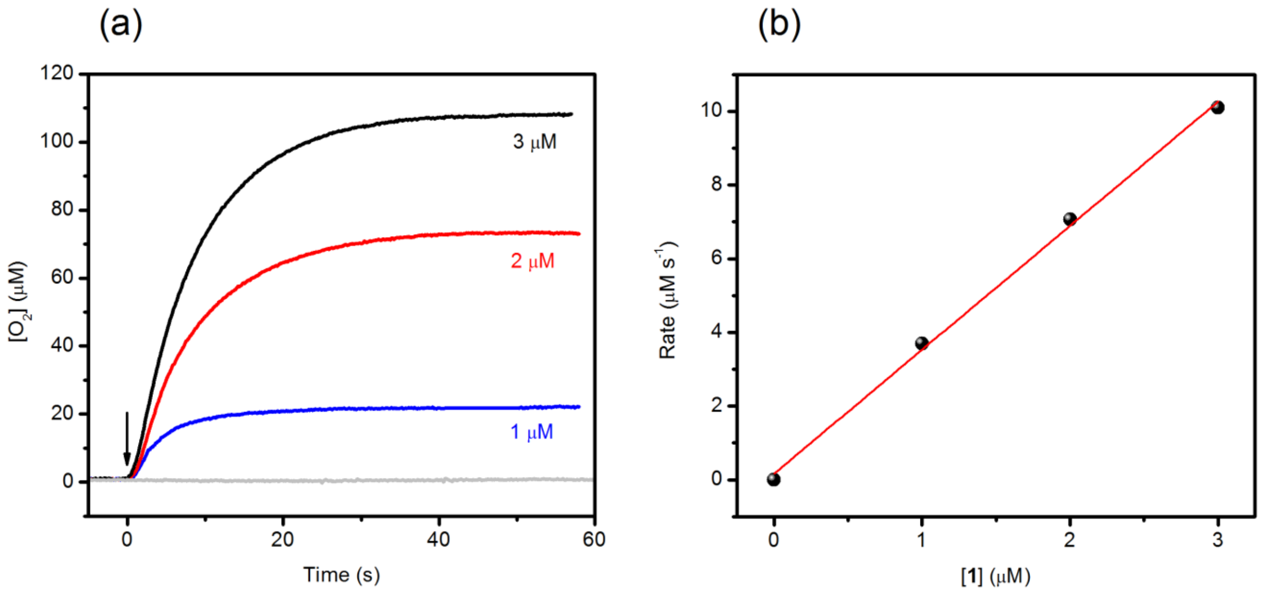

Fig. S6 $[Ru^{III}(bpy)_3](ClO_4)_3$-induced (1 mM) water oxidation experiments in borate buffer (0.1 M, pH = 8) using **1** as the catalyst. (a) Oxygen evolution traces obtained after addition of **1** (variable amount) to the solution of $[Ru^{III}(bpy)_3](ClO_4)_3$. Background is shown in grey. Arrow indicates the moment of addition of **1**. (b) Rate of the oxygen evolution as a function of the catalyst concentration.

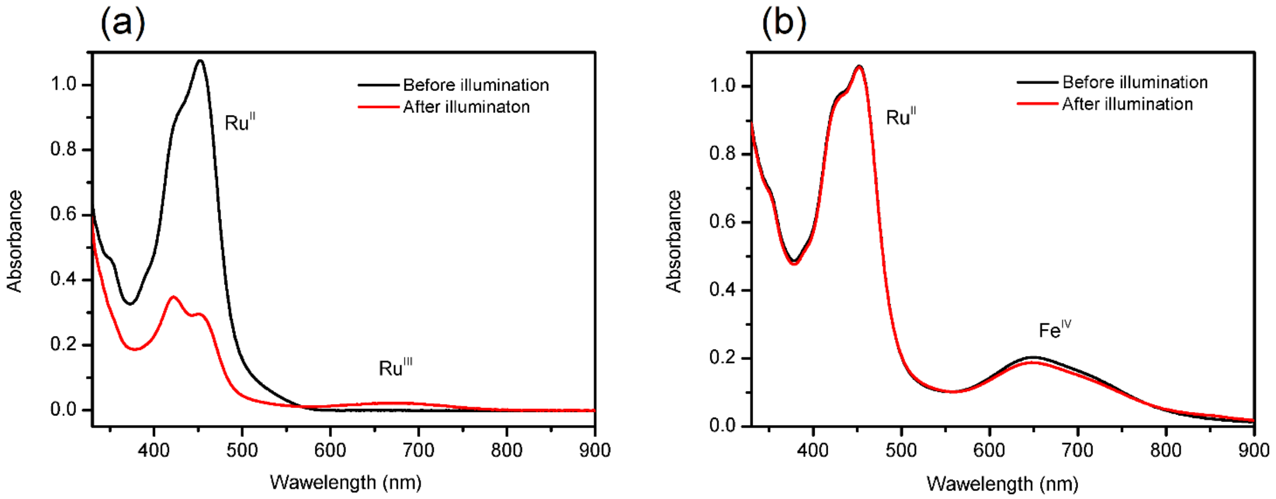

Fig. S7 (a) Steady-state UV-Vis absorption spectrum of the solution containing $[Ru(bpy)_3](ClO_4)_2$ (0.1 mM), $Na_2S_2O_8$ (1 mM) in borate buffer (pH 8.0) (black). After illumination of the cuvette at 450 nm (LEDs) during 10 s, the spectrum was recorded showing oxidation of Ru^{II} to Ru^{III} (red).

(b) The spectra of the solution containing $[Ru(bpy)_3](ClO_4)_2$ (0.1 mM), $Na_2S_2O_8$ (1 mM), and **1** (0.02 mM) in borate buffer (pH 8.0) before and after illumination. Accumulation of Ru^{III} is not observed. Decrease in intensity of the band at 650 nm indicates oxidation of Fe^{IV} to Fe^{V} shown in Figure 4 in the main text.

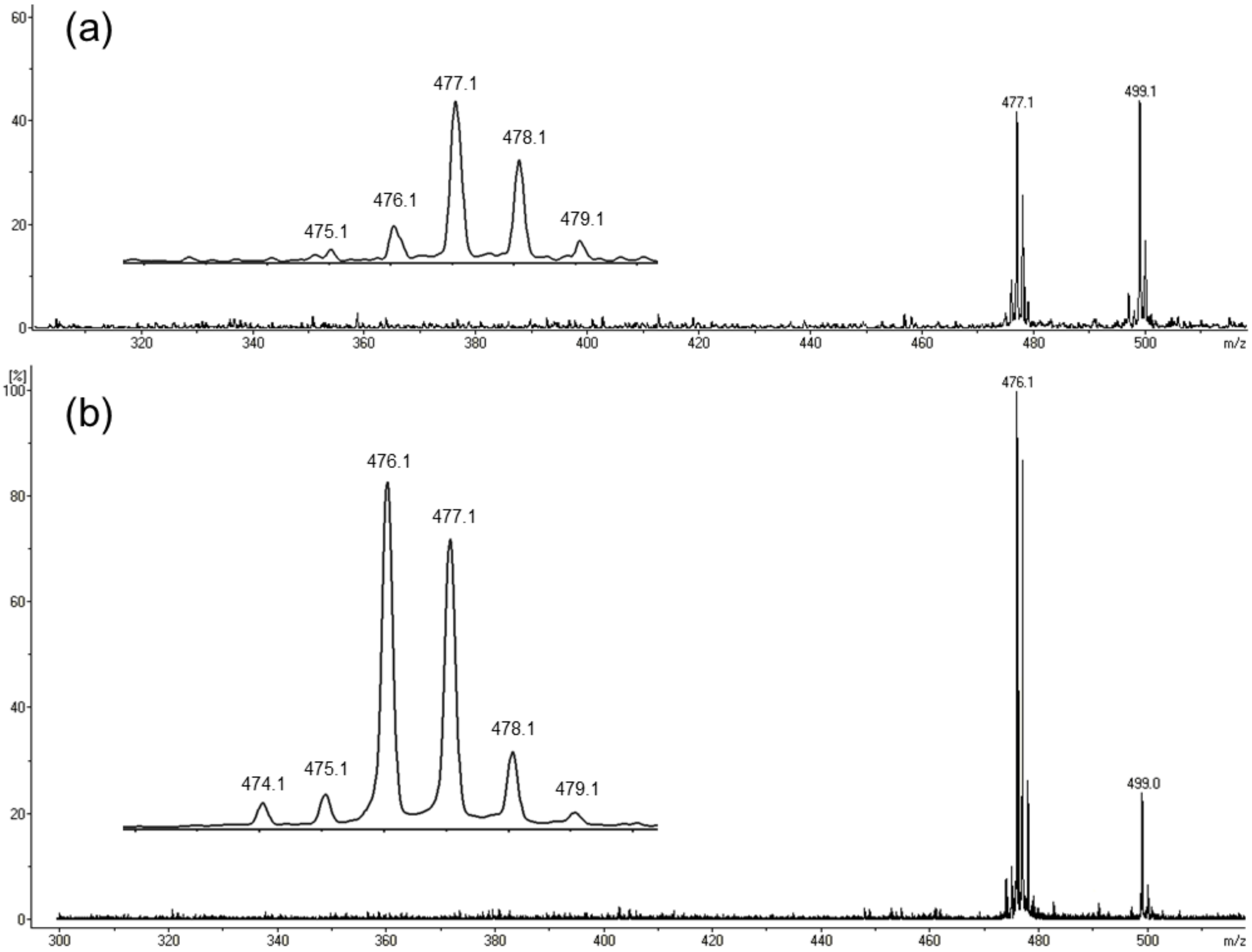

Fig. S8 ESI mass spectra of the catalytic system containing $[Ru(bpy)_3](ClO_4)_2$ (0.2 mM), $Na_2S_2O_8$ (2 mM), and **1** (2 μM) obtained in darkness in the negative ionization mode: (a) before photocatalysis; (b) after ca. 100 turnovers performed under illumination with LEDs at 450 nm during 30 s. The peaks at m/z = 477 and 499 correspond to $\{[Fe^{IV}(L\text{-}6H)]^{2-}+H^+\}^-$ and $\{[Fe^{IV}(L\text{-}6H)]^{2-}+Na^+\}^-$ respectively. The peak at m/z = 476 emerged in the spectrum (b) can be assigned to the active species $[Fe^{V}(L\text{-}6H)]^-$.

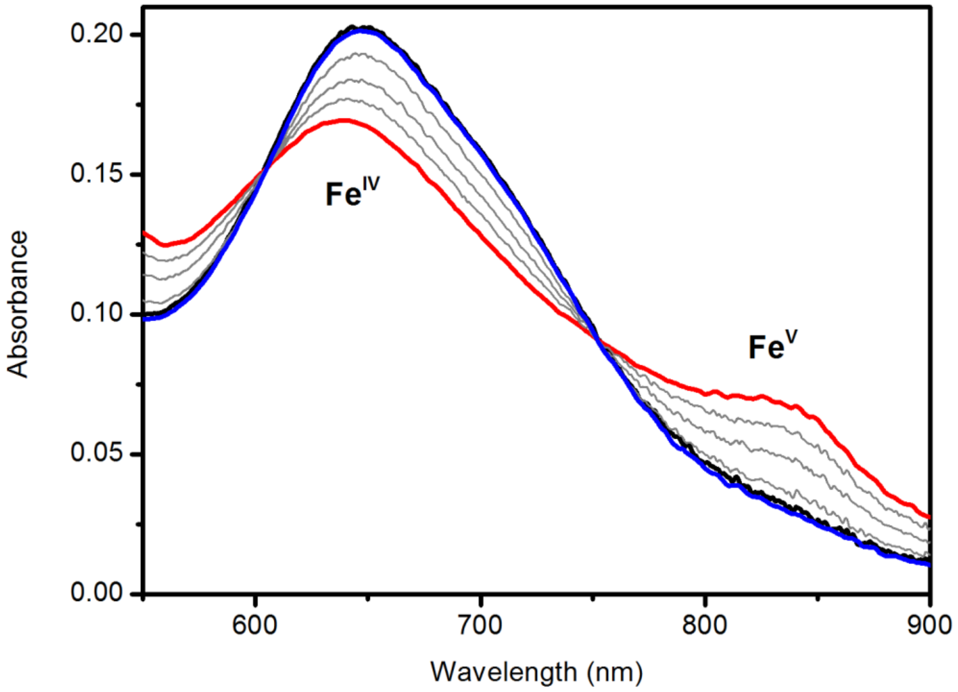

Fig. S9 UV-Vis spectra of the solution of **1** (3 ml, 0.02 mM) in borate buffer (pH 8.0) before (black), directly after (red) addition of $[Ru^{III}(bpy)_3](ClO_4)_3$ (0.06 μmol), and in 20 minutes (blue). Spectra shown in grey were recorded in 1, 5 and 10 minutes after the addition of $[Ru^{III}(bpy)_3](ClO_4)_3$ showing re-reduction of Fe^{V} to Fe^{IV}.

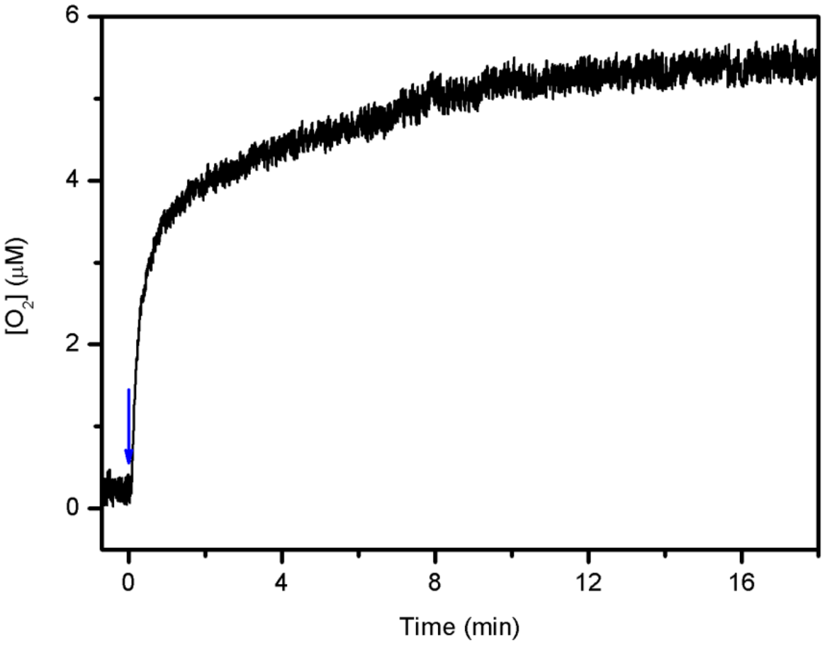

Fig. S10 Oxygen evolution trace obtained after addition of the equimolar amount of $[Ru^{III}(bpy)_3](ClO_4)_3$ to the solution of **1** (1 ml, 0.02 mM). Blue arrow indicates the moment of addition of $[Ru^{III}(bpy)_3](ClO_4)_3$. A fast oxygen evolution phase takes place during the first minute after addition of $[Ru^{III}(bpy)_3](ClO_4)_3$. This is followed by a slow phase that correlates with the regeneration of the Fe^{IV} species occurring over 15-20 min, observed by UV-Vis spectroscopy as shown in Fig. S9.

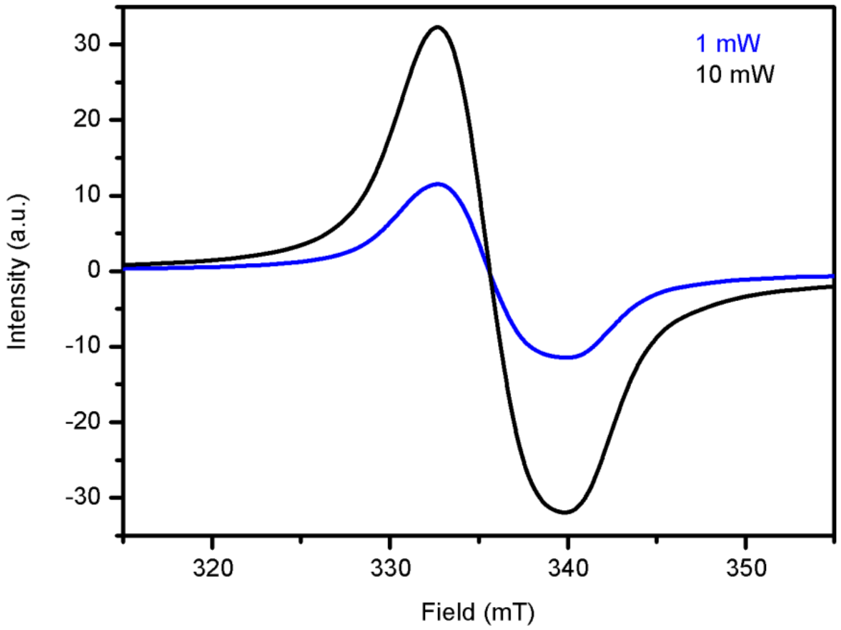

Fig. S11 EPR spectra of the solution containing **1** (0.2 mM), $[Ru(bpy)_3](ClO_4)_2$ (0.5 mM) and $Na_2S_2O_8$ (2 mM) frozen (5 K) after illumination at 450 nm. Increase of the microwave power from 1 mW to 10 mW leads to an increase of the EPR signal intensity by a factor of $\approx \sqrt{10}$ indicating that paramagnetic center is metal ion.

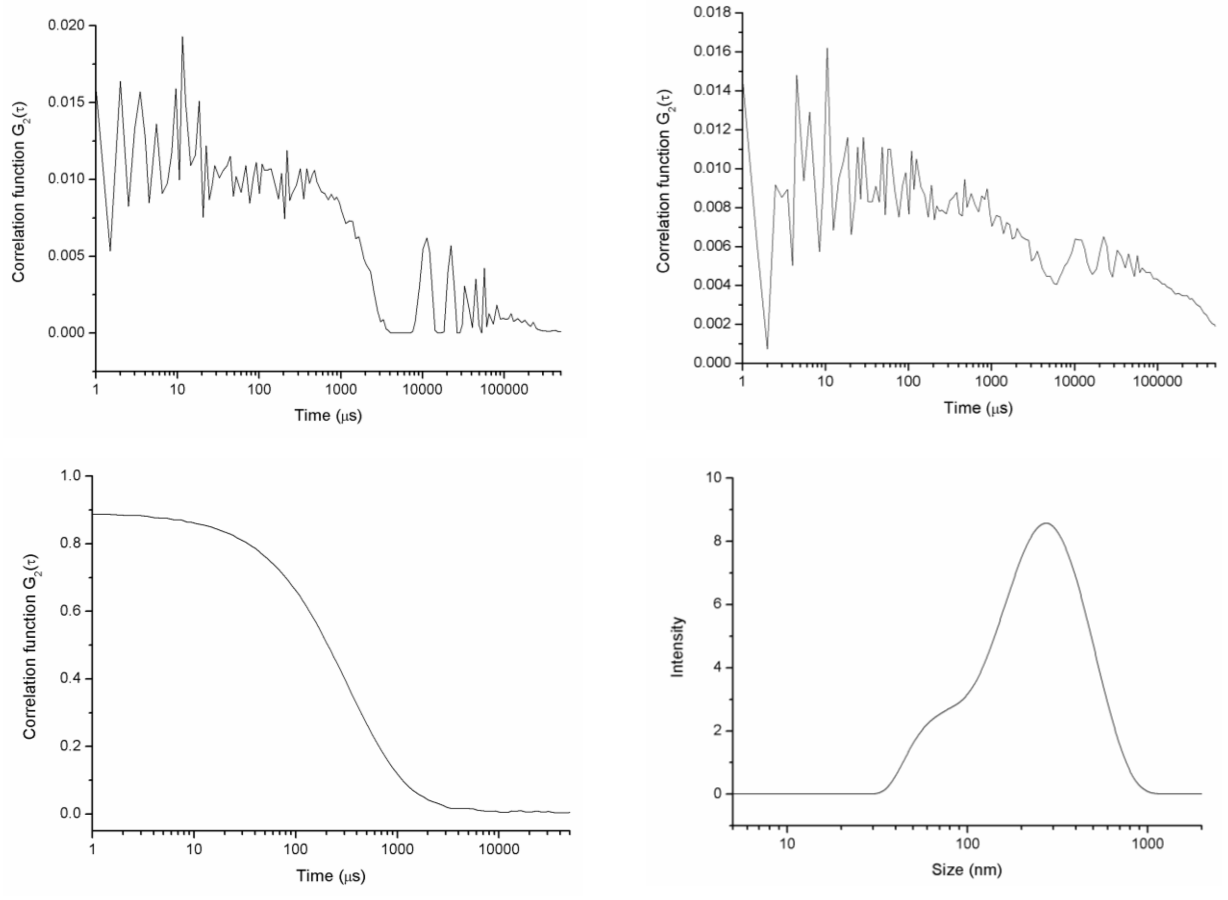

Fig. S12 Dynamic light scattering (DLS) experiments performed on the catalytic system and $Fe(ClO_4)_3$ for comparison. Top left: Correlation function as a function of time for the solution containing $[Ru(bpy)_3](ClO_4)_2$ (0.2 mM), $Na_2S_2O_8$ (2 mM), and **1** (0.02 mM) in borate buffer (pH 8.0). No particles are observed (y-Interception = 0.120) [6-7]. Top right: Correlation function for the same solution after illumination at 450 nm (LEDs) during 60 seconds. No particles are observed (y-Interception = 0.205). Bottom left: Correlation function for $Fe(ClO_4)_3$ (0.02 mM) dissolved in buffered water (pH 8.0) showing good light scattering (y-Interception = 0.942). Bottom right: Particles size distribution for the $Fe(ClO_4)_3$ solution.

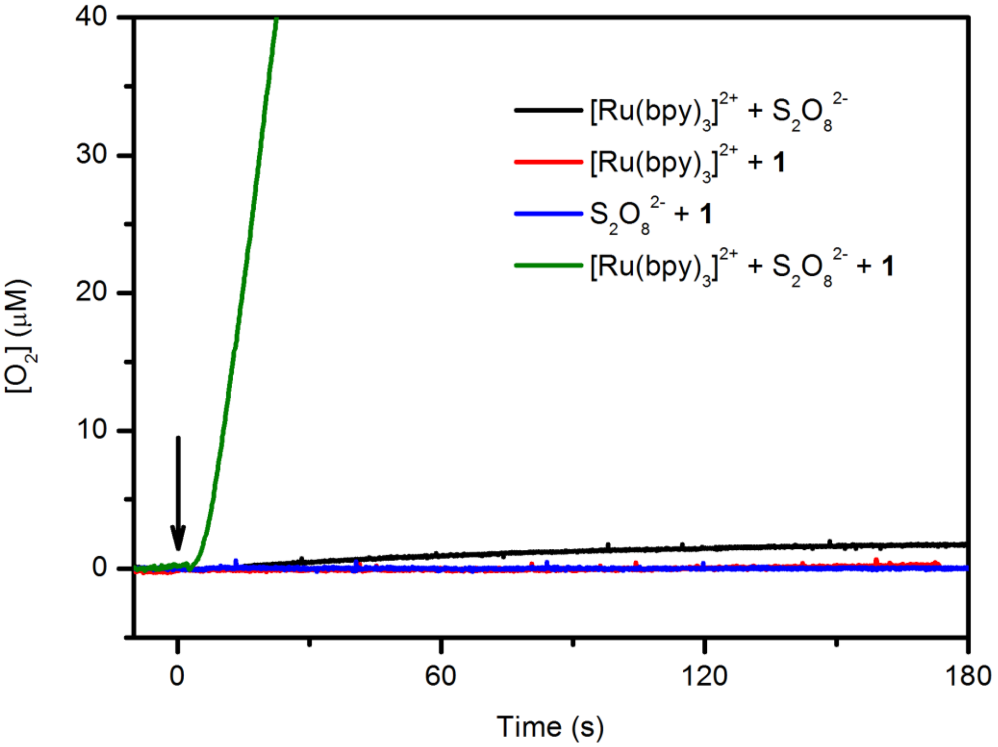

Fig. S13 Control experiments showing that oxygen is not evolved if the catalyst **1** (black curve), or the sacrificial electron acceptor (red curve), or the photosensitiser (blue curve) is absent. The oxygen evolution trace from the integral catalytic system is given for comparison (green curve). Arrow indicates start of illumination at 450 nm (LEDs). Concentration of components are as follows: $[Ru(bpy)_3](ClO_4)_2$ (0.2 mM), $Na_2S_2O_8$ (2 mM), **1** (1 μM) in borate buffer (0.1 M; pH 8.0).

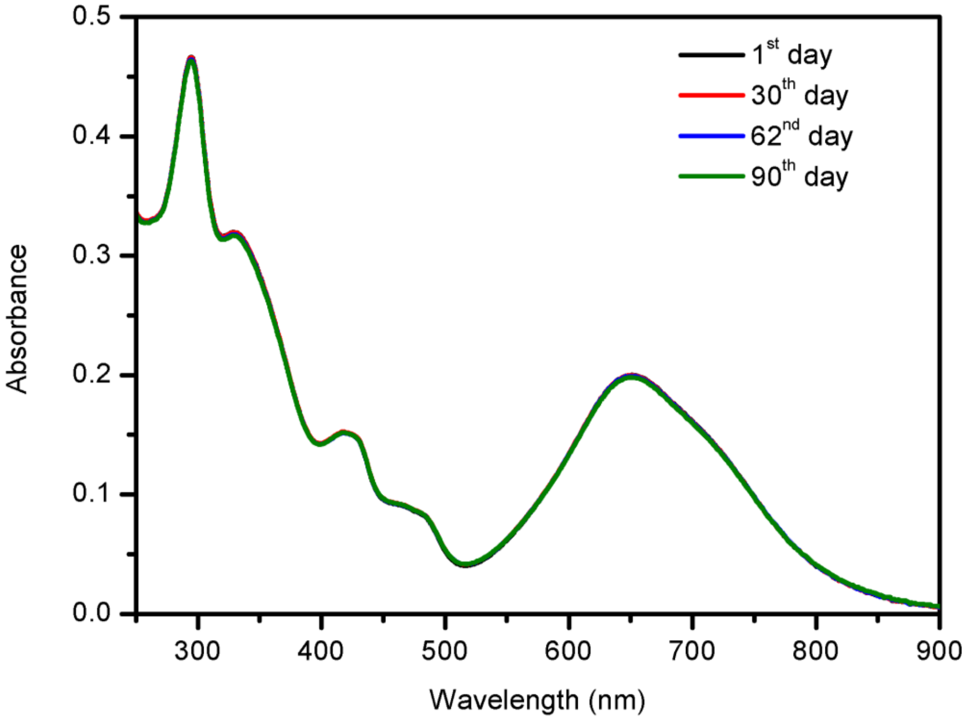

Fig. S14 UV-Vis absorption spectra of **1** (0.02 mM) in borate buffer (0.1 M) showing stability of the complex in aqueous solution at pH 8.0 over the period of 90 days.

References

1. V. Ya. Shafirovich, N. K. Khannanov and A. E. Shilov. *J. Inorg. Biochem.*, 1981, **15**, 113.
2. M. V. Pavliuk, E. Mijangos, V. G. Makhankova, V. N. Kokozay, S. Pullen, J. Liu, J. Zhu, S. Styring and A. Thapper, *ChemSusChem*, 2016, **9**, 2957.
3. M. Yamamoto, J. Föhlinger, J. Petersson, L. Hammarström and H. Imahori, *Angew. Chem. Int. Ed.*, 2017, **56**, 3329.
4. K. Lagarec and D. G. Rancourt, *Nucl. Instrum. Methods Phys. Res. B*, 1997, **129**, 266.
5. S. Tomyn, S. I. Shylin, D. Bykov, V. Ksenofontov, E. Gumienna-Kontecka, V. Bon and I. O. Fritsky, *Nat. Commun.*, 2017, **8**, 14099.
6. B. Das, A. Orthaber, S. Ott and A. Thapper, *ChemSusChem*, 2016, **9**, 1178.
7. L. D. Wickramasinghe, R. Zhou, R. Zong, P. Vo, K. J. Gagnon and R. P. Thummel, *J. Am. Chem. Soc.*, 2015, **137**, 13260.